PROCEEDINGS OF SCIENCE

Status of searches for rare kaon decays at NA62 & HIKE

Silvia Martellotti †

INFN LNF,
Via Enrico Fermi 54, 00044 Frascati, Italy

E-mail: silvia.martellotti@lnf.infn.it

Recent results from searches for rare kaon decays with the NA62 experiment at CERN are reported, together with the future prospects. A future experiment HIKE, to go beyond NA62, has been proposed to push kaon physics to an unprecedented frontier. The HIKE timescale and expected performance are described. Among the NA62 results, the measurement of the branching ratios of the flavour changing neutral current $K^+ \to \pi^+\mu^+\mu^-$ and the radiative non leptonic $K^+ \to \pi^+\gamma\gamma$ decays are reported, upper limits are given for lepton flavor and lepton number violating decays $K^+ \to \mu^-\nu e^+e^+$ and $K^+ \to \pi^-\pi^0 e^+e^+$. A search for new physics in the branching ratio of the decay $K^+ \to \pi^+e^+e^-e^+e^-$ is presented.

Workshop Italiano sulla Fisica ad Alta Intensità (WIFAI2023)
8-10 November 2023
Dipartimento di Architettura dell'Università Roma Tre, Rome, Italy

†Speaker on behalf of the NA62 Collaboration: A. Akmete, R. Aliberti, F. Ambrosino, R. Ammendola, B. Angelucci, A. Antonelli, G. Anzivino, R. Arcidiacono, T. Bache, A. Baeva, D. Baigarashev, L. Bandiera, M. Barbanera, J. Bernhard, A. Biagioni, L. Bician, C. Biino, A. Bizzeti, T. Blazek, B. Bloch Devaux, P. Boboc, V. Bonaiuto, M. Boretto, M. Bragadireanu, A. Briano Olvera, D. Britton, F. Brizioli, M.B. Brunetti, D. Bryman, F. Bucci, T. Capussela, J. Carmignani, A. Ceccucci, P. Cenci, V. Cerny, C. Cerri, B. Checcucci, A. Conovaloff, P. Cooper, E. Cortina Gil, M. Corvino, F. Costantini, A. Cotta Ramusino, D. Coward, P. Cretaro, G. D'Agostini, J. Dainton, P. Dalpiaz, H. Danielsson, M. D'Errico, N. De Simone, D. Di Filippo, L. Di Lella, N. Doble, B. Dobrich, F. Duval, V. Duk, D. Emelyanov, J. Engelfried, T. Enik, N. Estrada-Tristan, V. Falaleev, R. Fantechi, V. Fascianelli, L. Federici, S. Fedotov, A. Filippi, R. Fiorenza, M. Fiorini, O. Frezza, J. Fry, J. Fu, A. Fucci, L. Fulton, E. Gamberini, L. Gatignon, G. Georgiev, S. Ghinescu, A. Gianoli, M. Giorgi, S. Giudici, F. Gonnella, K. Gorshanov, E. Goudzovski, C. Graham, R. Guida, E. Gushchin, F. Hahn, H. Heath, J. Henshaw, Z. Hives, E.B. Holzer, T. Husek, O. Hutanu, D. Hutchcroft, L. Iacobuzio, E. Iacopini, E. Imbergamo, B. Jenninger, J. Jerhot, R.W. Jones, K. Kampf, V. Kekelidze, D. Kereibay, S. Kholodenko, G. Khoriauli, A. Khotyantsev, A. Kleimenova, A. Korotkova, M. Koval, V. Kozhuharov, Z. Kucerova, Y. Kudenko, J. Kunze, V. Kurochka, V. Kurshetsov, G. Lanfranchi, G. Lamanna, E. Lari, G. Latino, P. Laycock, C. Lazzeroni, M. Lenti, G. Lehmann Miotto, E. Leonardi, P. Lichard, L. Litov, P. Lo Chiatto, R. Lollini, D. Lomidze, A. Lonardo, P. Lubrano, M. Lupi, N. Lurkin, D. Madigozhin, I. Mannelli, A. Mapelli, F. Marchetto, R. Marchevski, S. Martellotti, P. Massarotti, K. Massri, E. Maurice, A. Mazzolari, M. Medvedeva, A. Mefodev, E. Menichetti, E. Migliore, E. Minucci, M. Mirra, M. Misheva, N. Molokanova, M. Moulson, S. Movchan, M. Napolitano, I. Neri, F. Newson, A. Norton, M. Noy, T. Numao, V. Obraztsov, A. Okhotnikov, A. Ostankov, S. Padolski, R. Page, V. Palladino, I. Panichi, A. Parenti, C. Parkinson, E. Pedreschi, M. Pepe, M. Perrin-Terrin, L. Peruzzo, P. Petrov, Y. Petrov, F. Petrucci, R. Piandani, M. Piccini, J. Pinzino, I. Polenkevich, L. Pontisso, Yu. Potrebenikov, D. Protopopescu, M. Raggi, M. Reyes Santos, M. Romagnoni, A. Romano, P. Rubin, G. Ruggiero, V. Ryjov, A. Sadovsky, A. Salamon, C. Santoni, G. Saracino, F. Sargeni, S. Schuchmann, V. Semenov, A. Sergi, A. Shaikhiev, S. Shkarovskiy, M. Soldani, D. Soldi, M. Sozzi, T. Spadaro, F. Spinella, A. Sturgess, V. Sugonyaev, J. Swallow, A. Sytov, G. Tinti, A. Tomczak, S. Trilov, M. Turisini, P. Valente, B. Velghe, S. Venditti, P. Vicini, R. Volpe, M. Vormstein, H. Wahl, R. Wanke, V. Wong, B. Wrona, O. Yushchenko, M. Zamkovsky, A. Zinchenko.

© Copyright owned by the author(s) under the terms of the Creative Commons
Attribution-NonCommercial-NoDerivatives 4.0 International License (CC BY-NC-ND 4.0).

PoS(WIFAI2023)027

1. The NA62 experiment

With the main goal to measure the branching ratio (BR) of the ultra-rare $K^+ \to \pi^+\nu\bar{\nu}$ decay with a precision similar to the theoretical predictions, the NA62 experiment started to take physics data in 2016 and collected the world's largest data sample of K^+ decays. The NA62 experiment is located at the CERN SPS and is operating with a 75 GeV/c hadron beam with a 6% K^+ component. A schematic view of the NA62 detector layout in the XZ plane is shown in Fig. 1, a detailed description of the detector and the beamline can be found in [1]. Simultaneously with the trigger conditions required for the $K^+ \to \pi^+\nu\bar{\nu}$ analysis [2] a few additional trigger lines are used [3] to select different event topologies. The incoming Kaons are identified by a differential Cherenkov counter (KTAG) with $\sigma \sim 70$ ps time resolution and the kaon momenta are measured by a three-station silicon pixel beam-spectrometer (GTK). A magnetic spectrometer (STRAW) measures the momenta and directions of charged particles produced in K^+ decays in a 75 m long fiducial volume, from 105 to 180 m downstream of the target. A Ring Image Cherenkov detector (RICH) provides a trigger time with $\sigma \sim 70$ ps time resolution and is optimized for the identification of positively charged particles [4]. The presence of signals in the quadrants of the CHOD (Charged particle Hodoscope) is used as a trigger condition. Particle identification is also provided by a quasi-homogeneous calorimeter (LKr) and a muon detector (MUV). A photon veto system includes the LKr and twelve ring-shaped lead-glass detectors (LAV1–12), together with two small angle shashlik calorimeters, IRC and SAC.

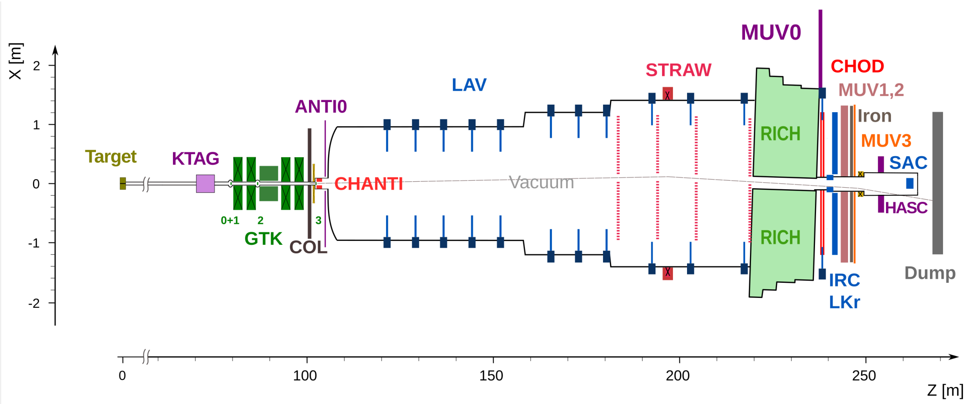

Figure 1: Schematic view of the NA62 detector layout in XZ plane.

2. Search for $K^+ \to \pi^+\mu^+\mu^-$ and $K^+ \to \pi^+\gamma\gamma$ decays

The dominant contributions to the flavour-changing neutral current decays such as $K^+ \to \pi^+\mu^+\mu^-$ are mediated by a virtual photon exchange ($K^\pm \to \pi^\pm\gamma^* \to \pi^\pm\ell^+\ell^-$) and involve long-distance hadronic effects described by a vector interaction form factor. Studies of the decay form factors contribute to experimental tests of lepton flavour universality [5][6][7]. A sample of 2.8×10^4 $K^+ \to \pi^+\mu^+\mu^-$ candidates with negligible background was selected from the 2017–2018 NA62 data set (Fig.2 left). $K^+ \to \pi^+\pi^+\pi^-$ candidates from the same data sample are used for normalization. The model-independent branching fraction is measured to be $\mathrm{BR}(K_{\pi\mu\mu}) = (9.15 \pm 0.08) \times 10^{-8}$[8], a factor three more precise than the previous measurement (Fig.2 right). The size of the $K_{\pi\mu\mu}$ data

PoS(WIFAI2023)027

sample is the main factor limiting the precision of this analysis. The decay form factor is presented as a function of the squared dimuon mass. A measurement of the form factor parameters and their uncertainties is performed[8] using a description based on Chiral Perturbation Theory at O(p^6).

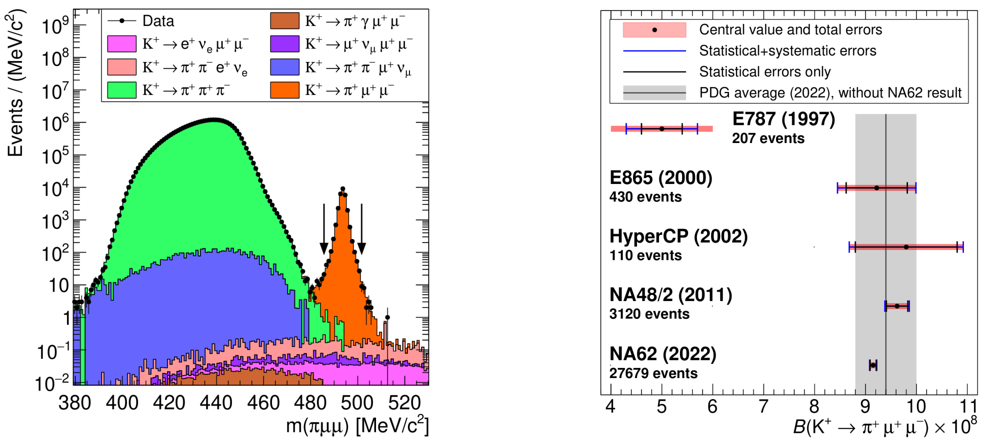

Figure 2: Left: reconstructed mass distributions m($\pi\mu\mu$) of events satisfying the signal selection for data (black markers) and simulated background and signal samples (filled areas). The arrows indicate the selected mass regions. The contribution from the simulated $K_{\pi\mu\mu}$ decays is scaled according to the PDG branching fraction [9]. Right: comparison with earlier measurements of the $K_{\pi\mu\mu}$ branching fraction, with the PDG [9] average shown as a shaded band.

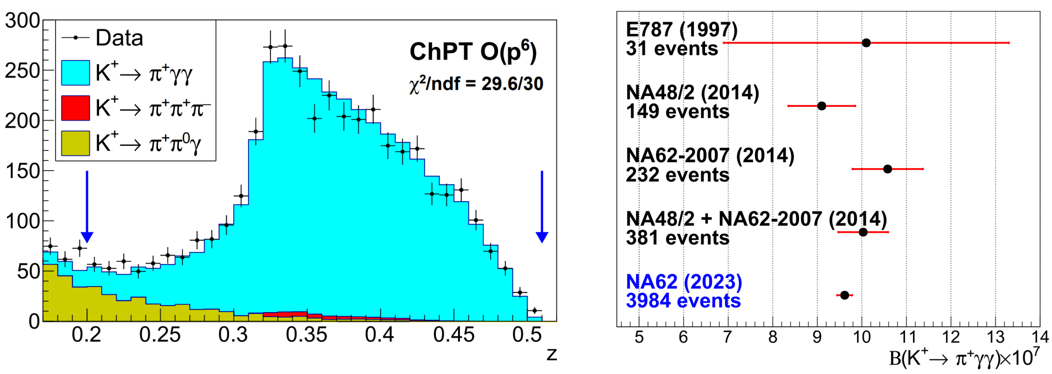

Figure 3: Left: distribution of $z = m^2_{\gamma\gamma}/m^2_K$ kinematic variable for selected $K^+ \to \pi^+\gamma\gamma$ candidates, for data (black markers) and simulated background and signal samples (filled areas). For the signal fit procedure ChPT O(p^6) assumption is adopted. The arrows mark the selected region. Right: summary of the branching fraction measurements in the ChPT O(p^6) framework. The error bars do not include uncertainties due to the external parameters of the ChPT fit.

Experimental studies of radiative non-leptonic kaon decays test chiral perturbation theory (ChPT), which describes low-energy QCD processes. For the $K^+ \to \pi^+\gamma\gamma$ decay, the ChPT description has been developed at both leading and next-to-leading orders [12][13][14]. A sample of 3984 candidates of the $K^+ \to \pi^+\gamma\gamma$ decay, with an estimated background of 291 ± 14 events, was selected from the 2017–2018 NA62 data set (Fig.3 left). The abundant $K^+ \to \pi^+\pi^0$ decay followed

PoS(WIFAI2023)027

by the prompt $\pi^0 \to \gamma\gamma$ decay is used for normalisation. In order to describe the observed di-photon mass spectrum, the next-to-leading order contribution in ChPT was found to be necessary. The decay branching ratio in the full kinematic range is measured to be $\mathrm{BR}(K_{\pi\gamma\gamma}) = (9.61 \pm 0.17) \times 10^{-7}$ [10] (Fig.3 right). For the ChPT test with $K^+ \to \pi^0 e^+ \nu\gamma$ decay search at NA62 see [11].

3. Search for $K^+ \to \mu^- \nu e^+ e^+$ and $K^+ \to \pi^- \pi^0 e^+ e^+$ decays

The $K^+ \to \mu^- \nu e^+ e^+$ decay is forbidden in the SM by either lepton number (LN) or lepton flavor (LF) conservation, depending on the flavour of the emitted neutrino. Strong evidence for the Majorana nature of the neutrino would be provided by the observation of lepton number violating (LNV) processes, including kaon decays [15, 16]. Furthermore, lepton flavour violating (LFV) kaon decays are expected in new physics models involving flavour violating Axion-like particles (ALPs) and Z′ particles [17, 18]. A search for the forbidden decay $K^+ \to \mu^- \nu e^+ e^+$ has been performed using the 2016–2018 NA62 data (Fig.4 left). The background in the signal region is estimated to be $N_B = 0.26 \pm 0.04$, where the uncertainty is dominated by the MC statistical contribution. The signal acceptance evaluated with simulations, assuming a uniform phase space distribution of signal events, is $A_{\mu\nu ee} = 0.0144$. The uncertainty in $A_{\mu\nu ee}$ is negligible for the purpose of the signal search. The single event sensitivity, defined as the branching fraction of the $K_{\mu\nu ee}$ decay corresponding to the observation of one signal event, is found to be $B_{SES} = (N_K \cdot A_{\mu\nu ee})^{-1} = (3.53 \pm 0.12) \times 10^{-11}$. No data events are observed in the signal region after unmasking. An upper limit on the signal BR is evaluated using the quantity B_{SES} and the numbers of expected background events and observed data events using the CL_S method [19]: $\mathrm{BR}(K^+ \to \mu^- \nu e^+ e^+) < 8.1 \times 10^{-11}$ at 90% CL [20].

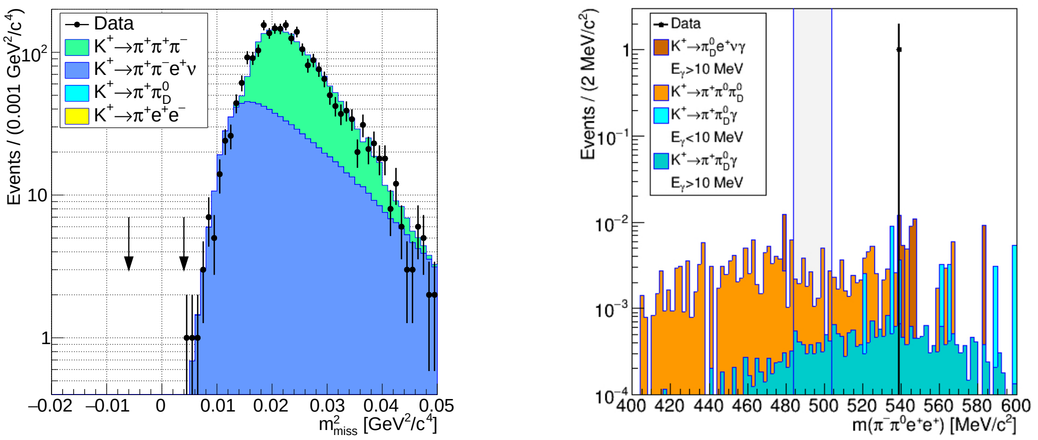

Figure 4: Left: reconstructed m^2_{miss} spectra for the data (black dots) and MC background samples (filled areas) obtained with the $K^+ \to \mu^- \nu e^+ e^+$ selection. The signal mass region is indicated by vertical arrows. Right: reconstructed $m_{\pi\pi ee}$ spectra of the data and simulated backgrounds obtained using the $K^+ \to \pi^- \pi^0 e^+ e^+$ selection. The $K^+ \to \pi^+ \pi^0 e^+ e^-$ contribution is the smallest, and is not shown. The shaded vertical band indicates the signal $m_{\pi\pi ee}$ region masked during the analysis.

The existing experimental limits on $K^+ \to \pi^- \ell^+ \ell^+$ decays lead to stringent constraints on active-sterile mixing angles amongst Majorana neutrinos. Below the kaon mass, these constraints are competitive with those obtained from neutrinoless double beta decays [21–23]. A search for

PoS(WIFAI2023)027

the forbidden decay $K^+ \to \pi^-\pi^0 e^+e^+$ has been performed using the 2016–2018 NA62 data set (Fig.4 right). One data event is observed in the control region, in agreement with the background expectation. The total expected background in the signal region is found to be $N_B = 0.044 \pm 0.020$, where the uncertainty is dominated by the statistical error in the pileup background estimate. After unmasking, no data events are found in the signal region. The signal acceptance evaluated with simulation assuming a uniform phase space distribution is $A^{LNV}_{\pi\pi ee} = (0.271 \pm 0.003)\%$. The uncertainty is due to the $\pi^0 \to \gamma\gamma$ decay reconstruction. The single event sensitivity is evaluated as $B_{SES} = (N_K \cdot BR_{\gamma\gamma} \cdot A^{LNV}_{\pi\pi ee})^{-1} = (3.68 \pm 0.12) \times 10^{-10}$, where $BR_{\gamma\gamma}$ is the $\pi^0 \to \gamma\gamma$ branching fraction[25]. An upper limit on the signal branching fraction is evaluated using the CL$_S$ method: BR$(K^+ \to \pi^-\pi^0 e^+e^+) < 8.5 \times 10^{-10}$ at 90% CL[24]. This result represents the first experimental limit on this decay rate.

4. Search for $K^+ \to \pi^+e^+e^-e^+e^-$ decay

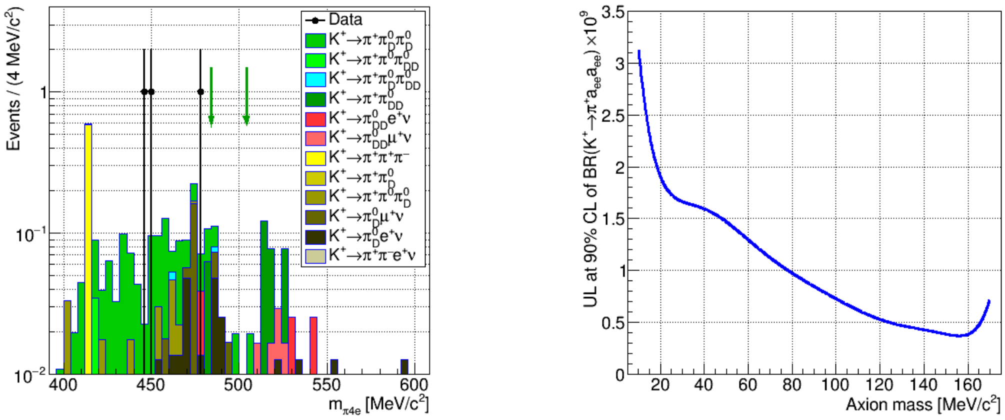

Figure 5: Left: reconstructed five-track mass spectra for data (black dots) and simulated samples (filled areas) after the $K\pi 4e$ selection. The signal region is shown with pairs of vertical arrows. Right: upper limit at 90% CL of the branching ratio of the prompt decay chain $K^+ \to \pi^+ aa, a \to e^+e^-$ as a function of the assumed axion mass.

Dark-sector models provide plausible dark-matter candidates and represent a compelling new-physics direction to explore [26, 27]. In the kaon sector, the process of particular interest is $K \to \pi XX$ followed by prompt $X \to e^+e^-$ decays, leading to characteristic multi-electron final states. Since this process has not been studied experimentally so far, O(10^{-6}) sensitivity to its BR is sufficient to improve existing constraints on dark-sector models. With the 2017–2018 data set, NA62 performed the first search for ultra-rare decay $K^+ \to \pi^+e^+e^-e^+e^-$ (Fig.5 left). The BR of the process is predicted in the Standard Model to be $(7.2 \pm 0.7) \times 10^{-11}$. The estimate of the total background in the signal region, validated by agreement of the data with simulation in the control regions, is $N_B = 0.18 \pm 0.14$. No data events are observed in the signal region after unmasking. Upper limits at 90% CL on the signal branching ratio is computed using the CL$_S$ method: BR$(K^+ \to \pi^+e^+e^-e^+e^-) < 1.4 \times 10^{-8}$ [28]. With this result, upper limits at 90% CL are obtained at the level of 10^{-9} for the BR of two prompt decay chains involving pair production

PoS(WIFAI2023)027

of hidden sector mediators: $K^+ \to \pi^+ aa(a \to e^+e^-)$, $K^+ \to \pi^+ S(S \to A'A', A' \to e^+e^-)$ (Fig:5 right).

5. HIKE experiment for future Kaon Physics

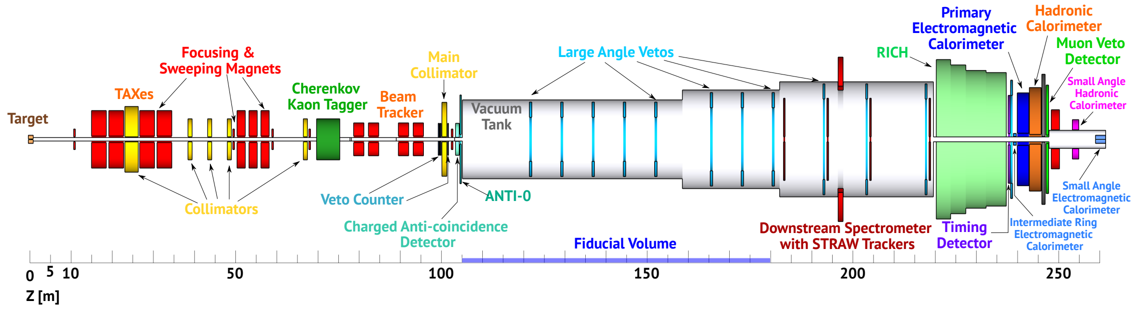

Figure 6: Schematic layout of the HIKE experimental setup during phase 1 (charged kaon beam).

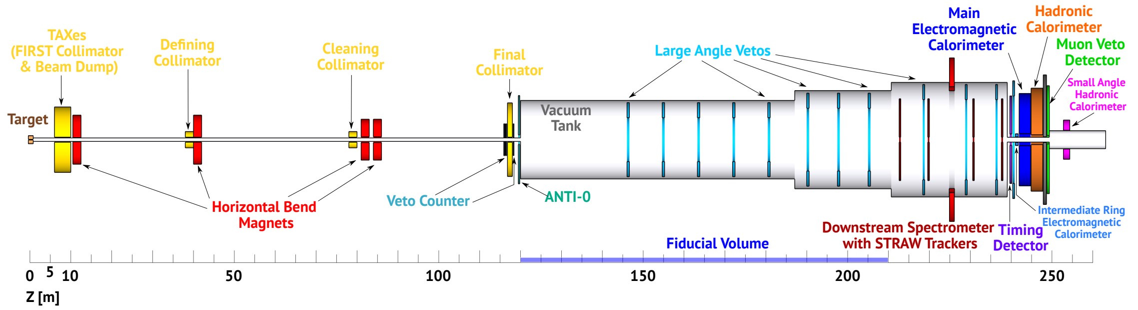

Figure 7: Schematic layout of the HIKE experimental setup during phase 2 (neutral kaon beam).

NA62 will take data till the long shutdown of 2026, in 2023 the proposal to extend Kaon physics at CERN to a new level of sensitivity has been published as the new High Intensity Kaon Experiment (HIKE)[29]. An integrated program with multiple phases: phase 1 with charged K^+ beam and phase 2 with K_L neutral beam, exploiting the high intensity beam line in the CERN North Area. HIKE phase 1 is estimated to start in 2031 after major beamline upgrades with a maximum possible beam intensity of 1.2×10^{13} POT/spill, which is 4 times the NA62 nominal intensity. This will result in a total of 2×10^{13} kaon decays in fiducial volume per year. With the final data sample expected to be 8 times larger than that of NA62 the main goal to measure BR($K^+ \to \pi^+ \nu\bar{\nu}$) at 5% precision will be reached. Appropriate modifications to the current setup to cope with higher intensity have been designed, a 4 times improvement in the time resolution with respect to NA62 is required. A schematic layout of HIKE phase 1 is shown in Fig.6. Technological solutions exist for all detectors and the challenges are aligned with HL-LHC projects and future flavor/dark matter experiments. In the HIKE phase 2, a neutral beam will be realized through a major upgrade to the NA48 beam line. The maximum possible beam intensity is expected to be 2×10^{13} POT/spill corresponding to about 3.8×10^{13} K_L decays in the fiducial volume per year. The main HIKE phase 2 physics goal is the measurement of the BR($K_L \to \pi^0 \ell^+ \ell^-$) at 20% precision. For the neutral phase the beam tracker will be removed and some detectors reconfigured, the schematic layout is shown in Fig.7.

PoS(WIFAI2023)027

References

[1] E. Cortina Gil et al, JINST 12 (2017) P05025 (2017).

[2] E. Cortina Gil et al, JHEP 06 (2021), 093.

[3] E. Cortina Gil et al, JHEP 03 (2023) 122.

[4] JINST 15 P10025 (2020).

[5] Nucl. Phys. B 291 (1987) 692.

[6] JHEP 08 (1998) 004.

[7] Phys. Part. Nucl. Lett. 5 (2008) 76.

[8] E. Cortina Gil et al, JHEP 11 (2022) 011.

[9] PDG, PTEP 2022 (2022) 083C01.

[10] arXiv:2311.01837v1.

[11] JHEP 09 (2023) 040.

[12] Nucl. Phys. B303 (1988) 665.

[13] Phys. Lett. B386 (1996) 403.

[14] Nucl. Phys. B730 (2005) 1.

[15] Phys. Lett. B 491 (2000) 285.

[16] Phys. Rev. D 71 (2005) 113014.

[17] J.High Energy Phys. 01 (2020) 158.

[18] Rep. Prog. Phys. 86 (2023) 016201.

[19] A.L. Read, J. Phys. G 28 (2002) 2693.

[20] Physics Letters B 838 (2023) 137679.

[21] Phys. Rev. D71 (2005) 113014.

[22] JHEP 05 (2009) 030.

[23] JHEP 02 (2018) 169.

[24] PLB 830 (2022) 137172.

[25] Phys. Lett. B788 (2019) 552.

[26] J. Phys. G 47 (2020) 010501.

PoS(WIFAI2023)027

[27] Eur. Phys. J. C 81 (2021) 11.

[28] PLB 846 (2023) 138193.

[29] CERN-SPSC-2023-031.

PoS(WIFAI2023)027